AGEOSTROPHIC CONTRIBUTIONS TO A NON-CONVECTIVE HIGH WIND EVENT IN THE GREAT LAKES REGION

Joshua D. Durkee
Meteorology Program, Department of Geography and Geology,
Western Kentucky University
Bowling Green, KY

Christopher M. Fuhrmann
Department of Geography, University of North Carolina at Chapel Hill
Chapel Hill, NC

John A. Knox*
Department of Geography, University of Georgia
Athens, GA

John D. Frye
Department of Geography & Geology, University of Wisconsin-Whitewater
Whitewater, WI

Abstract

On 12-13 November 2003, a mid-latitude cyclone caused a widespread non-convective high wind event across the Great Lakes region. In this paper, we attempt to explain the dynamical cause for these winds using ageostrophic wind theory. First, the theory of ageostrophic winds is explored and related to some conventional rules of thumb for wind forecasting. Next, ageostrophic wind terms relating to the isallobaric wind, horizontal advective processes, vertical advective processes, and friction are calculated from the North American Regional Reanalysis. The aggregate total wind results for each region are compared to observed winds at three different pressure levels: 925, 850, and 700 hPa. The aggregate results are in good agreement with observations, particularly at lower altitudes in the Lake Erie region, lending credence to our approach. The dominant ageostrophic contributor to the high winds for this storm was the isallobaric wind, but all terms played non-negligible roles at one location, level, or time. Analyses that focus only on one term or do not vectorially combine all geostrophic and ageostrophic contributions are therefore likely to be misleading.

Revised for National Weather Digest
8 November 2011

Corresponding Author: Dr. John A. Knox
Department of Geography, University of Georgia, 210 Field St., Room 204, Athens, GA 30602. Email: johnknox@uga.edu

1. Introduction

High winds (Table 1) not associated with thunderstorms, tornadoes or tropical cyclones are deadly and damaging weather events that confront the operational forecasting community in most regions of the United States. Recent climatological research has demonstrated that, in a typical year in the United States, non-convective high winds are just as deadly as tropical cyclones, more deadly than thunderstorm winds, and account for more property and crop damage than thunderstorms or tornadoes (Table 2) (National Weather Service 2005; Lacke et al. 2007; Ashley and Black 2008). Knox et al. (2010) provides a comprehensive review of non-convective winds caused by extratropical cyclones. Below we summarize the aspects of this review article most relevant to operational forecasting, particularly in the Great Lakes region.

National Weather Service (NWS) High-Wind Criteria		
Wind Type	**Magnitude**	**Duration**
Sustained	18 m s^{-1}	≥ 1 hour
Gust	26 m s^{-1}	Any duration

Table 1. Typical National Weather Service criteria for high-wind watch or warning (from Lacke et al. 2007).

Event Type	Deaths	Injuries	Damages ($M)
High Wind	118	613	4093.0
Thunderstorm Wind	94	1394	1632.5
Tornado	225	4076	3700.8
Tropical Cyclone	123	1427	28,070.5

Table 2. Summary of Natural Hazard Statistics (http://www.weather.gov/os/hazstats.shtml) for 2000-2004. After Lacke et al. (2007).

Although the Northeast and West Coast regions exhibit the most fatalities from non-convective high winds (Ashley and Black 2008), those living in the Great Lakes region are also vulnerable to these events. According to Hubert and Morford (1987), wind ranks first or second among all weather elements responsible for fatalities or significant property/crop damage during the fall and winter in the Great Lakes region. Popular Great Lakes pastimes such as boating and other outdoor activities also account for 25% and 23% of all non-convective high wind fatalities across the contiguous United States, respectively (Ashley and Black 2008). Non-convective high wind events in the Great Lakes region can trigger seiches that cause fatalities and destruction on the water and along shorelines (Niziol and Paone 2000). For example, Pore et al. (1975) found that 94% of significant storm surges on Lake Erie at Buffalo occurred during the generally non-convective cold season of September-April. Taken together, these statistics indicate that Great Lakes residents are at serious risk from non-convective high wind events.

Forecasting non-convective high wind events can be a challenge, in part, because a comprehensive theory of their causes has yet to be fully articulated. Approximately 83% of all non-convective high wind fatalities nationally are attributable to extratropical cyclones (Ashley and Black 2008), supporting Niziol and Paone's (2000) results from a 20-year climatological analysis for Buffalo, NY. In a 44-year climatology, Lacke et al. (2007) found that non-convective high winds were generally associated with lower than normal sea-level pressures, and the highest gusts were generally associated with the lowest sea-level pressures. Furthermore, Lacke et al. (2007) determined that the direction of a non-convective high wind is from the southwest quadrant (i.e., winds from the south through west direction) at least 70% of the time, thereby extending Niziol and Paone's (2000) similar finding for Buffalo to the entire Great Lakes region and for a longer period of record. Recently, Asuma (2010) also found a similar southwest quadrant preference for non-convective windstorms in a climatological study focusing on the Northeast United States.

However, the ultimate causes of the high winds are still a matter of some debate. A number of hypotheses for the generation of non-convective high winds have been presented in the research literature, regional forecast discussions, and technical memoranda from the National Weather Service (NWS). These include strong surface pressure gradients and isallobaric winds associated with intensifying cyclones (Richwien 1980; Crupi 2004), mesoscale topographic/orographic channeling of high winds (Niziol and Paone 2000; Crupi 2004; Hultquist et al. 2006), and diabatic cooling in regions of enhanced mesoscale slantwise circulations (Browning 2004).

Other studies have attributed non-convective high winds to features and processes in the upper troposphere and lower stratosphere. Lacke et al. (2007) suggested that the chronic tendency for southwest quadrant non-convective high winds across the entire Great Lakes region implied a connection with mid-latitude cyclone dynamics rather than more local topographic causes. For example, tropopause folds (Reed 1990; Uccellini 1990) and intrusions of high-momentum, high-ozone air into the middle troposphere have been observed in the vicinity of high-velocity surface winds using satellite remote sensing techniques (Browning and Reynolds

1994; Iacopelli and Knox 2001). The transport of this air from the upper and mid-troposphere to the surface in the vicinity of strong cyclones has been related to weak static stability (Iacopelli and Knox 2001), negative buoyancy produced by evaporative cooling (Browning 2004), and strong vertical shear instabilities (Browning and Reynolds 1994). Mechanical turbulence associated with jet streak dynamics may also account for high-momentum air reaching the surface away from the cyclone center (Danielsen 1964), and even in cases where a cyclone is not present. For example, Pauley et al. (1996) noted that stratospheric air could be mixed to the surface via a combination of upper-level and boundary layer processes.

To help forecasters, Kapela et al. (1995) developed an operational forecast checklist (see Appendix in their study) for strong wintertime post-cold front winds across the northern Great Plains. Although the checklist identifies particular features and processes that are *associated* in space and time with non-convective high winds (e.g., strong pressure gradient, upper-level jet streak), what ultimately *causes* the high winds remains the subject of current research. Recently, Schultz and Meisner (2009) found that synoptic and mesoscale subsidence associated with a mid-latitude cyclone played a role in the wind and dust storm event in north Texas in 2007. Kurtz and Martinelli (2010) found directional preferences in non-convective high wind events in the north-central Plains that generally confirm Lacke et al.'s (2007) inference that mid-latitude cyclone dynamics are a primary factor. Asuma (2010) noted near dry-adiabatic lapse rates and strong planetary boundary layer wind speeds in the southwest quadrants of cyclones.

The purpose of this article is to help forecasters understand which processes contribute to non-convective high winds. First, we employ a self-consistent dynamical framework of ageostrophic wind that is based on, and extends, the work of Rochette and Market (2006; hereafter RM06) that provided an illustrative-but-not-exhaustive example of using ageostrophic wind concepts for a typical weather situation. This dynamical approach allows quantitative comparisons of isallobaric and advective processes with the geostrophic and frictional components. We then apply this approach to two different locations and times in a notable non-convective high wind event over the Great Lakes region on 12-13 November 2003 in order to determine the relative importance of various ageostrophic contributions to the observed wind.

2. Theory and Computation of Ageostrophic Wind

a. Ageostrophic wind equation

The crux of the problem in predicting non-convective winds is quantifying and forecasting the ageostrophic component of the horizontal wind near the surface, since the geostrophic component is generally well-forecast. When the ageostrophic component is large and has a large component parallel to the geostrophic wind, the strongest non-convective winds are likely to occur.

Following Haltiner and Martin (1957, p. 194) and in parallel with the discussion of RM06, the ageostrophic component of the wind for mid-latitude quasi-geostrophic background conditions as contributions from four physical processes is written as:

$$\mathbf{V}_{\mathbf{ag}} = \underbrace{\frac{1}{f}\mathbf{k}\times\frac{\partial \mathbf{V}_{\mathbf{g}}}{\partial t}}_{A} + \underbrace{\frac{V}{f}\mathbf{k}\times\frac{\partial \mathbf{V}_{\mathbf{g}}}{\partial s}}_{B} + \underbrace{\frac{w}{f}\mathbf{k}\times\frac{\partial \mathbf{V}_{\mathbf{g}}}{\partial z}}_{C} - \underbrace{\frac{1}{f}\mathbf{k}\times\mathbf{F}_{\mathbf{H}}}_{D}, \quad (1)$$

in which f is the Coriolis parameter, V is the horizontal wind speed, s indicates the downstream direction in natural coordinates, w is the vertical velocity, and F_H is the horizontal friction vector (mostly omitted in discussion provided by RM06). These four contributions to the ageostrophic wind vector can be identified as:

A: Isallobaric wind due to local pressure changes
B: Horizontal advective ageostrophic wind ("inertial-advective")
C: Vertical advective ageostrophic wind ("inertial-convective")
D: Ageostrophic wind due to friction

While Equation (1) is not new, it is important to stress that all contributions to the ageostrophic wind must be considered, and must be combined as a vectorial sum. Haurwitz (1946) warned that "the concept of the isallobaric wind has to be abandoned" because Term A in Equation (1) is not necessarily larger than the other terms. Nevertheless, it is not unusual for discussions of high wind events to focus primarily or exclusively on the isallobaric wind (e.g., Richwien 1980) or fail to sum vectorially the isallobaric wind with the other wind components (e.g., Crupi 2004). In the next section, we will attempt to quantify and add vectorially each of the four contributions for different stages of a notable Great Lakes windstorm.

b. Discussion of terms

Below we discuss some aspects of the terms in (1) that are not found in RM06 and/or that are relevant to this study.

1) Horizontal advective ageostrophic wind (Term B)

The horizontal advective term can be expanded into sub-terms related to downstream curvature and downstream wind-speed changes:

$$\underbrace{\frac{V}{f}\mathbf{k}\times\frac{\partial \mathbf{V_g}}{\partial s}}_{B}=\underbrace{-\frac{1}{f}\frac{V^2}{R}\mathbf{t}}_{B1}+\underbrace{\frac{1}{f}V\frac{\partial V}{\partial s}\mathbf{n}}_{B2} \tag{2}$$

in which R is the radius of curvature of trajectories, $\boldsymbol{t}$ is the tangential vector and $\boldsymbol{n}$ is the normal vector in natural coordinates (see Holton 2004, his Fig. 3.1). These sub-terms are better known as:

B1: Ageostrophic wind in gradient balance
B2: Ageostrophic wind due to diffluence/confluence

The vector directions of the two sub-terms indicate that sub-term B1 is in the same direction as the geostrophic wind, and causes either subgeostrophic or supergeostrophic winds (depending on the sign of R; subgeostrophic in troughs, supergeostrophic in ridges). In contrast, sub-term B2 is directed perpendicular to the geostrophic wind, to the left of $\mathbf{V_g}$ in the case of confluent flow.

In practice, application of (2) is a bit problematic. It is hampered by errors in the estimation of R due to replacing trajectories with streamlines (e.g., height contours). Holton (2004, p. 69) indicated that trajectories and streamlines are coincident only when the local rate of change of the wind direction vanishes. In this study we use the approximation (Knox 1996, p. 201)

$$R=\frac{\left(u^2+v^2\right)^{3/2}}{u\dfrac{dv}{dt}-v\dfrac{du}{dt}} \tag{3}$$

A side issue is the appropriateness of using the geostrophic wind instead of the full wind in the calculations of the terms (S. Jascourt 2009, personal communication). This is similar to the open question of whether to use the geostrophic wind or the total wind in calculations of symmetric and inertial instability; see Schultz and Knox (2007, Section 4). In the calculations here, we try both options by using both the geostrophic and full wind in the advective part of B1 and R; and both the geostrophic and full wind in B2, as well as in the calculations of Term C.

2) Vertical advective ageostrophic wind (Term C)

The vertical advection term generally has received less attention than the other contributions to the ageostrophic wind. Haltiner and Martin (1957) discussed its role only in the case of veering winds. RM06 limited their discussion to the magnitude of this term, not its direction. Saucier (1955, p. 246) commented that "this contribution easily can be as important as" the other terms. Its importance in tropopause fold situations, where high-speed winds may be brought relatively close to the Earth's surface, has not been investigated in-depth to our knowledge. RM06 did calculate this "inertial-convective term" for one case (their Fig. 16), finding it generally weak except near a trough and jet streak entrance region.

In veering (warm air advection), the cross-product in Term C has the same orientation as the vertically averaged horizontal flow. Hence, Term C leads to supergeostrophic winds for upward motion ($w > 0$) in veering flow (Fig. 1a).

The opposite is true for backing (i.e., cold air advection), which is the situation present for most, if not all, non-convective high wind events associated with mid-latitude cyclones. In backing conditions, the cross-product in Term C points in the opposite direction of the vertically averaged horizontal flow. However, for downward motion where $w < 0$ (as shown in Fig. 1b), the direction of the ageostrophic contribution is the same as that of the vertically averaged horizontal flow. Therefore, *supergeostrophic winds can occur in cold air advection when air is sinking*. Since sinking motion is consistent with cold air advection in quasi-geostrophic dynamics (in the absence of strong positive vorticity advection) and in cold frontal dynamics (Bluestein 1993, p. 336), then this discussion supports the observation that non-convective winds can be maximized following cold frontal passage, i.e., in cold air advection (Kapela et al. 1995). This effect should also be magnified in the presence of high-speed winds in the vicinity of a tropopause fold.

One other forecasting rule of thumb may be explicable via the vertical advection term. For purposes of surface wind forecasting, it is said that wind profiles with unidirectional shear lead to higher surface winds than do profiles in which the wind direction changes markedly from the surface on up (Kapela et al. 1995, p. 235). In such circumstances, the vertical shear vector is oriented in the same direction as the wind. The cross-product in Term C would then point to the left of the wind vectors, and so would Term C in the case of upward motion (Fig. 1c). Since simple approximations of friction

also lead to an ageostrophic wind directed to the left of the geostrophic wind in the Northern Hemisphere (Saucier 1955, p. 242), the result is that Terms C and D are mostly additive in the case of unidirectional shear, but the two terms are generally much less synergistic for either backing or veering conditions. To the extent that friction and downward advection of momentum are the two dominant ageostrophic forcing terms in a given situation, therefore, *unidirectional shear is likely to maximize the ageostrophic wind in situations of rising motion*. This may help explain the rule of thumb and its efficacy in daytime situations (although we have so far omitted discussion of the effect of turbulent mixing).

Fig. 1(a)

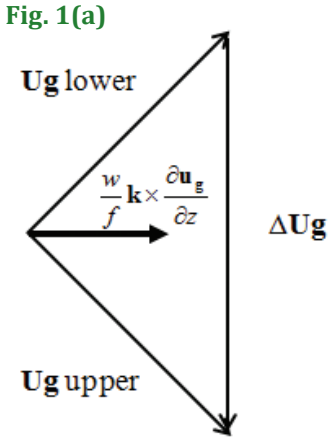

Fig. 1(b)

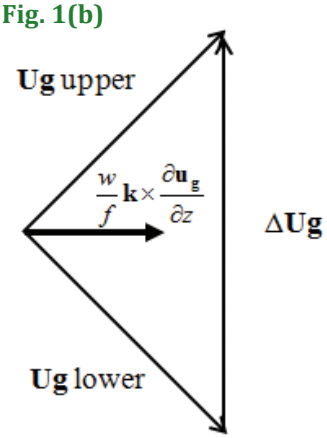

Fig. 1. The vector (bold arrow) of the vertical advection contribution to the ageostrophic wind (Term C in Equation 1) in a) veering, b) backing, and c) unidirectional shear conditions. The vertical advection term therefore points in the same general direction as the vertically averaged mean flow in the case of a) upward motion for veering conditions, and b) downward motion for backing conditions. In c), the vertical advection term points to the left of the geostrophic wind, similar to the direction of the frictional term.

Fig. 1(c)

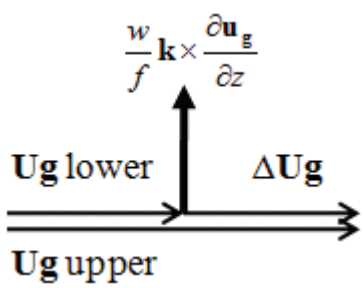

3) Frictional ageostrophic wind (Term D)

The turbulent eddy effects in Term D cannot be represented exactly, owing to the turbulence closure problem (e.g., Stull 1988, ch. 6). For research on high near-surface winds in which mixing would presumably be maximized, an appropriate approximation would seem to be the well-mixed boundary layer (Holton 2004, pp. 123-124). In this approximation, the two components of ageostrophic wind due to boundary-layer turbulence can be written as a coupled set of equations:

$$u_{ag} = -v\kappa_S\sqrt{u^2+v^2} \tag{4}$$

$$v_{ag} = u\kappa_S\sqrt{u^2+v^2} \tag{5}$$

in which

$$\kappa_S = \frac{C_{DN}}{fh} \tag{6}$$

where C_{DN} is the aerodynamic drag coefficient in statically neutral conditions and h is the boundary-layer height; and

$$u \equiv u_g + u_{ag}; v \equiv v_g + v_{ag} \tag{7}$$

Because of (7), the set of equations (4)-(5) is not only coupled, it is also nonlinear and cannot be solved algebraically. For the calculations presented in the next section, numerical solution of (7) using the Broyden (1965) method was performed. Drag coefficients were calculated using estimates of roughness lengths from Stull (1988, p. 380) and an altitude-dependent formula for C_{DN} as a function of altitude (Stull 1988, p. 266). Using 1/e = .3678 for the von Kármán constant (Bergmann 1998), $C_{DN} = 2 \times 10^{-3}$ at 925 hPa over land and 7.5×10^{-4} at 925 hPa over water for our case. These values yield physically realistic values of frictional ageostrophic wind using data for our case (as demonstrated in Section 4).

This approach to calculating Term D is qualitatively similar to the simple linear frictional drag approach pioneered by Guldberg and Mohn (e.g., Djurić 1994, pp. 108-109), but it is more sophisticated since it incorporates concepts of turbulent flux.

3. Data Sources

This study utilized a variety of meteorological and climatological data. Individual storm reports of damaging non-convective high winds for the period 12-13 November 2003 over the Midwest and Great Lakes regions were obtained using the Storm Events Database from the National Climatic Data Center (NCDC, http://www.ncdc.noaa.gov/oa/climate/sd/). This database serves as a search function for hazardous weather reports within *Storm Data*, a monthly publication from NCDC (online at:

http://www7.ncdc.noaa.gov/IPS/sd/sd.html).

Surface and upper-air meteorological variables over the Midwest and Great Lakes regions used to calculate wind-related variables were diagnosed using data from the North American Regional Reanalysis (NARR, http://www.emc.ncep.noaa.gov/mmb/rreanl/; Mesinger et al. 2006). The NARR was developed through the National Centers for Environmental Prediction (NCEP) and is a long-term, dynamically consistent, data-assimilation-based collection of climate data for North America from 1979 to the present. The NARR was produced with high spatial (32 km), vertical (45 layers) and temporal (3 hourly) resolution and is based on the April 2003 frozen version of NCEP's mesoscale Eta forecast model and data assimilation system, (EDAS; Mesinger et al. 2006). Analysis of meteorological variables from the NARR analyses for 12-13 November 2003 was performed using the General Meteorological Package (GEMPAK, http://www.unidata.ucar.edu/software/gempak/) software.

4. Storm Overview

On 12-13 November 2003, an intensifying mid-latitude cyclone tracked across the Midwest and Great Lakes regions. Convective complexes in the warm sector of the cyclone produced four tornadoes, two of which resulted in two deaths and three injuries in eastern Ohio, as well as large hail and damaging thunderstorm winds. Nearly $500,000 in property damage was reported across portions of the Ohio River Valley from convective storms during this event (NCDC 2003).

Of greater consequence, however, were the post-frontal non-convective high winds that occurred in association with the intensifying cyclone. These non-convective high winds, with gusts over 38 m s^{-1}, contributed to eight deaths and 23 injuries (NCDC 2003). These winds also helped produce one of the largest seiches in recent history on Lake Erie (Great Lakes Environmental Research Laboratory 2006). Property and crop damage estimates from the non-convective high winds totaled $36 million and were reported primarily across the Great Lakes region. Damages exceeding $1 million were reported in counties across central Iowa, southeast Lower Michigan, northern Ohio, and southeast Pennsylvania. Most notably, the bulk of the damage ($21 million) was experienced in southeast Lower Michigan. Across other parts of Lower Michigan, non-convective wind damages associated with the cyclone were so severe that a local utility company called it the worst windstorm since the *Edmund Fitzgerald* storm in 1975 (Hultquist et al. 2006), while a state park in northern Lower Michigan reported the most tree damage from a single storm since the Armistice Day storm in 1940 (NCDC 2003; Knox 2004).

An impressive aspect of this storm was the longevity and spatial extent of high wind reports (Fig. 2; Tables 3 and 4). These winds occurred in a variety of locations with respect to surface and upper-level wind features, offering an opportunity to compare the relative contributions of different forcing mechanisms to the observed wind field at different stages and locations during the storm.

In this article we examine two different locations and stages (Fig. 3). The first stage centers on southeast Lower Michigan and Lake Erie at 0300 UTC 13 November. Fig. 4 depicts the synoptic conditions at 0300 UTC over the Great Lakes region. A 990-hPa cyclone was present near Sault Ste. Marie, MI with a surface ridge upstream across the Upper Midwest (Fig. 4a). These features resulted in a strong isallobaric gradient extending east and northeast from Wisconsin and Ohio into southern Ontario, with southwest isallobaric winds over much of Lower Michigan (Fig. 4b). Cold air advection was also occurring upstream

Time (Day/ UTC)	KSBN		KLAN		KFNT		KTOL		KDTW		KCLE		KERI	
	5-Min. Avg.	Max. Gust	5-Min. Avg.	Max. Gust	5-Min. Avg.	Max. Gust	5-Min. Avg.	Max. Gust	5-Min. Avg.	Max. Gust	5-Min. Avg.	Max. Gust	5-Min. Avg.	Max. Gust
12/12-15	6	N/A	4	N/A	4	N/A	4	N/A	4	N/A	6	N/A	6	8
12/15-18	10	12	7	9	3	N/A	8	10	9	10	7	8	7	8
12/18-21	12	14	10	12	4	N/A	8	12	10	12	8	11	8	11
12/21-00	15	22	17	**28**	10	13	15	19	15	21	13	16	8	11
13/00-03	17	23	17	25	15	22	**20**	**27**	**20**	24	**20**	**26**	13	19
13/03-06	17	22	15	20	16	22	17	23	**19**	24	18	24	**18**	24
13/06-09	14	18	15	19	**18**	22	15	21	15	21	15	23	14	21

Table 3. Maximum 5-minute average wind (m s-1) and maximum wind gust (m s-1) recorded at ASOS at South Bend, IN (KSBN), Lansing, MI (KLAN), Flint, MI (KFNT), Toledo, OH (KTOL), Detroit, MI (KDTW), Cleveland, OH (KCLE), and Erie, PA (KERI), during 3-hour increments from 1200 UTC 12 November 2003 through 0000 UTC 14 November 2003. Boldfaced values indicate winds that satisfied the NWS high-wind definition in Table 1. Underlined values indicate the maximum for each location for the 36-hour time period.

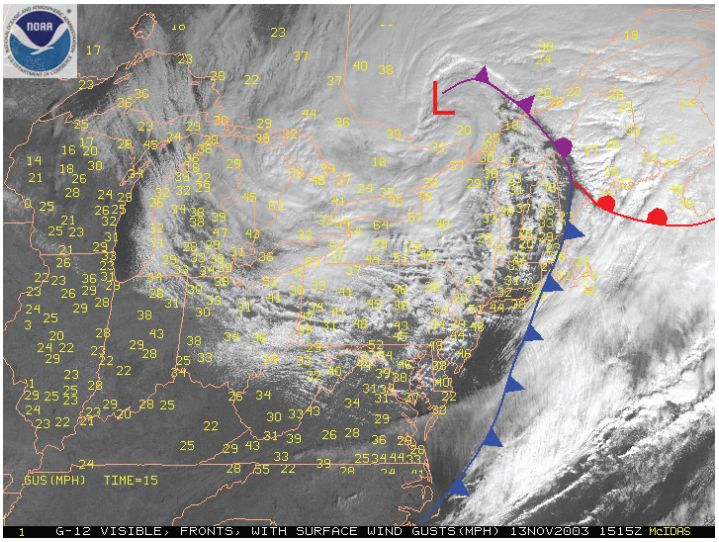

Fig. 2. Geostationary Operational Environmental Satellite (GOES)-12 visible satellite image with overlaid fronts and surface wind gusts (numbers, in mph) at 1515 UTC 13 November 2003. Image from http://www.ncdc.noaa.gov/img/climate/research/2003/nov/nestorm-pg.jpg.

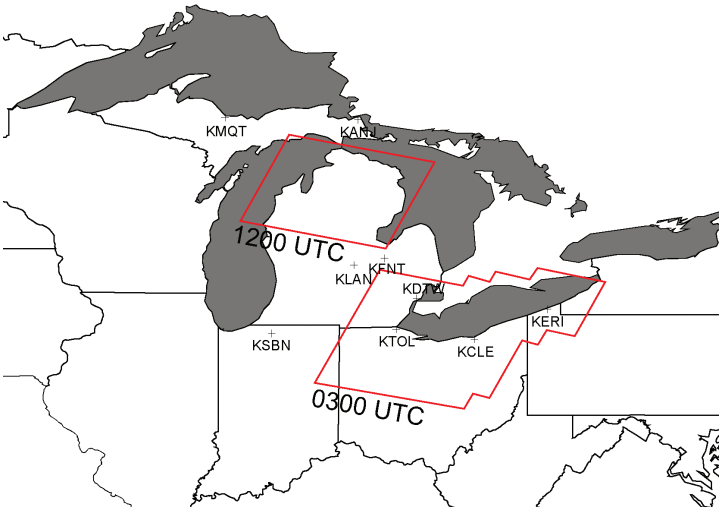

Fig. 3. The two domains and observation times examined in this analysis of the 12-13 November 2003 non-convective high wind event. NWS observing sites relevant to this study are labeled.

through a deep layer of the troposphere, as evidenced by strong winds (> 25 m s^{-1}) and cold temperatures (< -15°C) at 700 hPa across the Upper Midwest (Fig. 4c). At 500 hPa, a lobe of cyclonic vorticity was centered across Lower Michigan, implying anticyclonic vorticity advection in the region of cold air advection immediately upstream (Fig. 4d). The combined forcing of anticyclonic vorticity advection and cold air advection resulted in strong sinking motions extending from the Upper Midwest into the southern tier of Lower Michigan (Fig. 4e). At 300 hPa, a jet streak extended from the Great Plains to the Midwest with winds in the core of the jet exceeding 75 m s^{-1} (Fig. 4f). The cyclonically curved jet streak was associated with upper-level convergence to the west of the short-wave trough axis across western Michigan and Ohio, and with strong upper-level divergence in a diffluent region to the northeast of the short-wave trough axis. This is in general agreement with Moore and VanKnowe's (1992) modeling results for curved jet streaks.

The superimposed regions of upper-level and mid-level subsidence were coincident with a tropopause fold near the short-wave trough axis. Fig. 5 is a cross-section from the Upper Peninsula of Michigan to eastern Ohio (see inset of Fig. 5 for the exact locations) and depicts a tropopause fold (thick black lines) extending downward to

Time (UTC)	Location, County, State	Latitude	Longitude	Gust (m s^{-1})
0214	St. Clair, St. Clair County, Michigan	42.86	-82.55	29
0314	Charlevoix County, Michigan	N/A	N/A	27
0327	Maybee, Monroe County, Michigan	42.00	-83.52	26
0400	Akron, Summit County, Ohio	41.06	-81.51	26
0408	Empire, Leelanau County, Michigan	44.82	-86.80	34
0500	Erie County, Pennsylvania	N/A	N/A	31
0548	Flint WJRT TV Channel 12, Genesee County, Michigan	42.80	-83.75	37
0616	Saginaw Harry Browne Airport, Saginaw County, Michigan	43.43	-83.86	26
0629	Pellston, Emmet County, Michigan	45.55	-84.78	28
0717	Pontiac, Oakland County, Michigan	42.64	-83.29	26
0756	Bad Axe, Huron County, Michigan	43.80	-83.00	26
1048	Presque Isle County, Michigan	N/A	N/A	35
1300	Presque Isle Lighthouse, Erie County, Pennsylvania	N/A	N/A	32
1400	Port Hope, Huron County, Michigan	43.94	-82.71	26
1448	Erie County, Pennsylvania	N/A	N/A	28

Table 4. Maximum high-wind gust (m s^{-1}) observations for 13 November 2003 as recorded in NCDC's Storm Event Database.

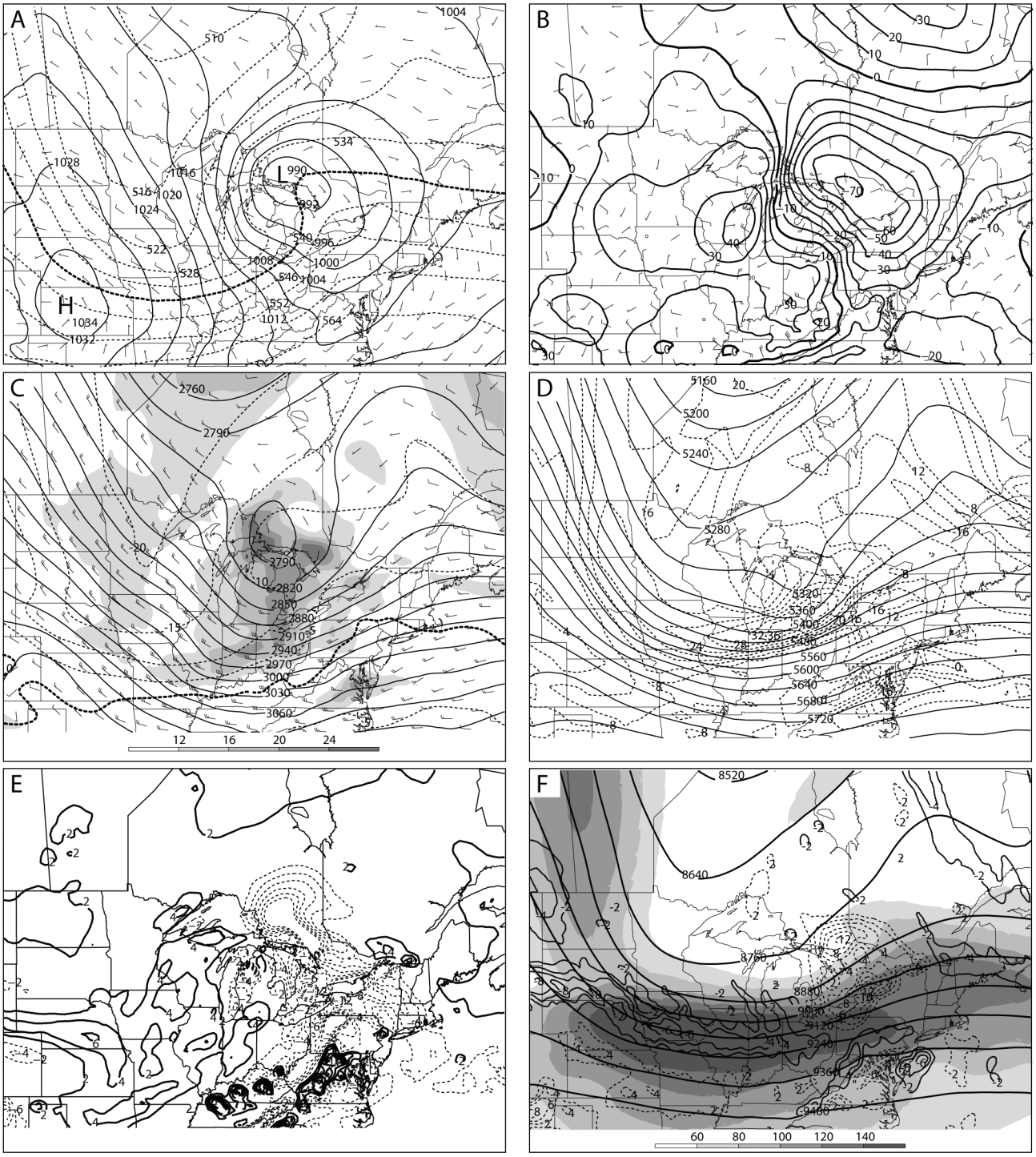

Fig. 4. Synoptic conditions at 0300 UTC 13 November 2003:

(a) Sea-level pressure (solid lines, hPa), 1000-500 hPa thickness (dashed lines, dkm), and wind vectors (standard barbs in m s^{-1});

(b) 925-hPa height changes (m 3-h^{-1}) and isallobaric wind vectors (standard barbs); (c) 700-hPa heights (solid lines, m), temperature (dashed lines, °C), wind vectors (standard barbs), and absolute vorticity ≥ 12 x 10^{-5} s^{-1} (shading);

(d) 500-hPa heights (solid lines, m) and absolute vorticity (dashed lines, 10^{-5} s^{-1});

(e) Omega (ω) at 700-hPa where ω > 0 is downward vertical motion (solid lines) and ω < 0 is upward vertical motion (dashed lines);

(f) 300-hPa heights (thick solid lines, m), convergence (bold solid lines, 10^{-5} s^{-1}), divergence (thin dashed lines, 10-5 s^{-1}), and wind speed ≥ 60 kt, or 30 m s-1 (shading legend units in knots).

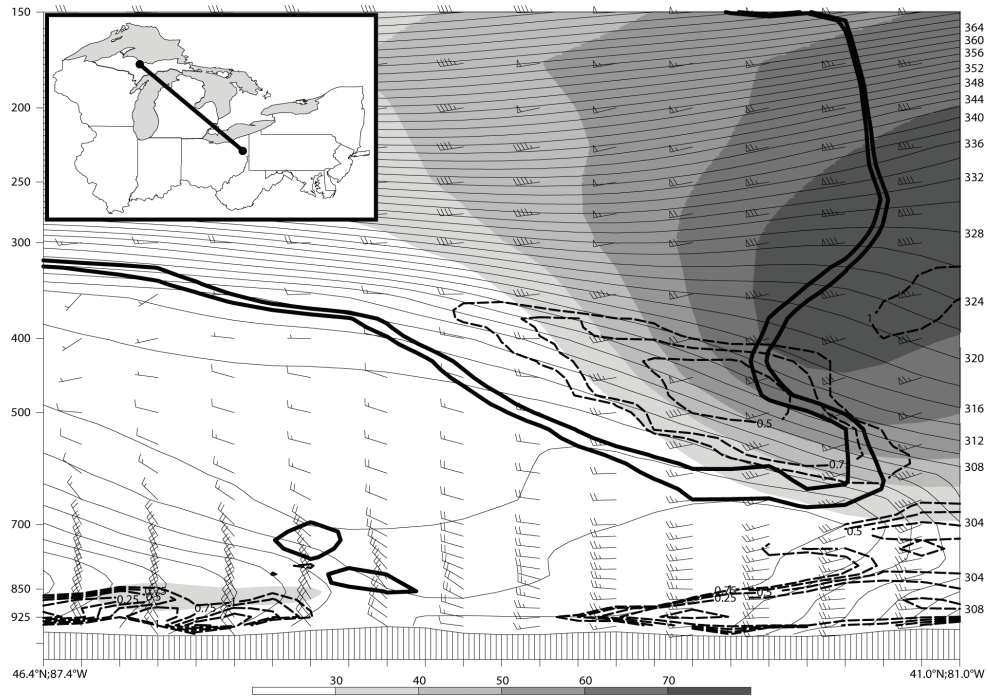

Fig. 5. Vertical cross-section from Marquette, MI (left) to Youngstown, OH (right; see inset for locations) at 0300 UTC 13 November 2003 showing moist isentropes (i.e., θ_{es}, thin solid lines, K), wind vectors (standard barbs in m s^{-1}), wind speed ≥ 30 m s^{-1} (shading), potential vorticity values of 1.5 and 2.0 PVU (thick solid lines), and bulk Richardson values ≤ 1.0 (dashed lines).

nearly 700 hPa over Ohio. Small values of the Richardson number (dashed lines) were collocated with the fold. The implications of this for the observed surface wind field are explored in the following section.

The second stage focuses on northern Lower Michigan at 1200 UTC 13 November. Figure 6 depicts the synoptic conditions at this time, including the deepening of the surface cyclone to 982 hPa (Fig. 6a) and large near-surface height rises in its wake over northern Lower Michigan, which reversed the direction of the isallobaric wind versus 0300 UTC (Fig. 6b). Strong northwesterly winds and 700-hPa cold air advection were also present over the region (Fig. 6c).

Compared to the first stage, upper-level synoptic conditions during the second stage were markedly different. A lobe of positive vorticity at 500 hPa was located south and east of the Great Lakes (Fig. 6d) while relatively weak vertical velocities at 700 hPa were evident across Lower Michigan and the Upper Midwest (Fig. 6e). The 300-hPa jet streak was now displaced well to the south across the Ohio River Valley and Mid-Atlantic region (Fig. 6f). The 1200 UTC 13 November sounding from Gaylord, MI (not shown) revealed an absence of high-momentum air in the mid-to-upper troposphere over northern Lower Michigan (wind speeds between 500 hPa and 300 hPa < 20 m s^{-1}). Although the upper-level dynamics were far from weak owing to the strongly cyclonically curved flow aloft, there was no strong jet streak and no tropopause fold in the vicinity of northern Lower Michigan at 1200 UTC.

5. Results

Composite geostrophic and ageostrophic contributions to the wind were calculated at 700, 850 and 925 hPa for 119 points in the Lake Erie region (Fig. 7) and 56 points in northern Lower Michigan (Fig. 8) for 0300 and 1200 UTC on 13 November 2003, respectively. Unlike RM06, we did not apply smoothing to the model output before performing the calculations. Calculations were performed for terms B1, B2, and C using both geostrophic (GEO; Figs. 7 and 8 left columns) and total wind (WND; Figs. 7 and 8 right columns) as discussed in Section 2, in order to compare the accuracy of the two approaches.

At 700 hPa, the isallobaric component (A) and horizontal advective contributions (B1 and B2) compose the majority of the ageostrophic wind at both stages of the storm. In the Lake Erie Region (Fig. 7a), the vertical advective term (C = 2.9 m s^{-1}) is more than 50% of the magnitude of each of the other three terms (A = 4.9 m s^{-1}, B1 = 4.9 m s^{-1}, B2 = 1.4 m s^{-1}) and is nearly an order of magnitude larger than in northern Lower Michigan at 700 hPa. This is also the approximate level at which the base of the tropopause fold is found (see Fig. 5).

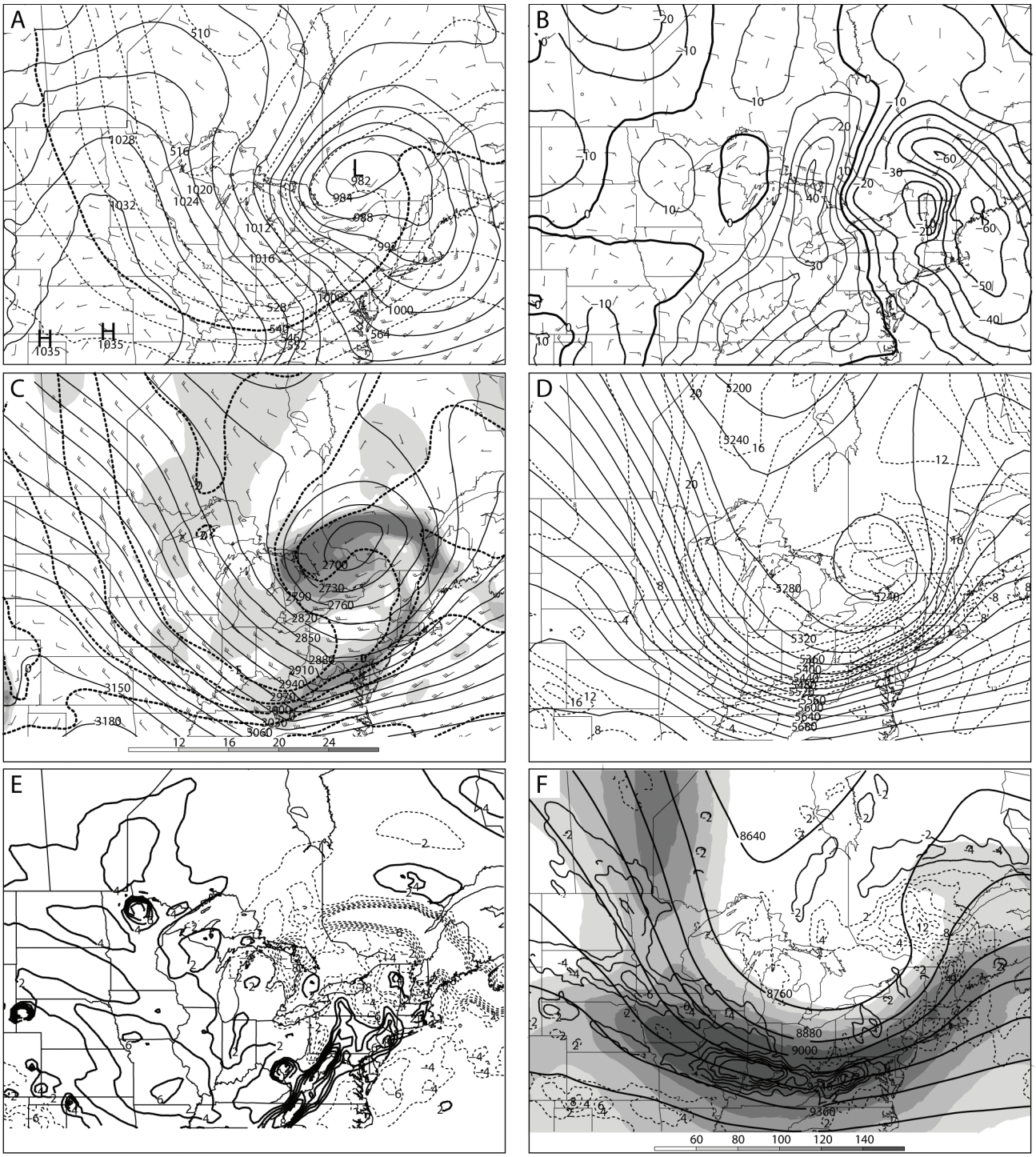

Fig. 6. As in Figure 4 except for northern Lower Michigan at 1200 UTC. 13 November 2003.

As discussed earlier, one hypothesis for the generation of non-convective high winds is the transport of high-momentum air associated with a tropopause fold via mechanical turbulence. To determine the potential for turbulent mixing, Richardson numbers less than 1 were plotted along the cross-section in Fig. 5. These values indicate the presence of Kelvin-Helmholtz instability (Stull 1988, pp. 176-178), and suggest possible small-scale mixing near, below, and downstream of the tropopause fold. Richardson values less than 1 below 850 hPa in Fig. 5 were likely the result of boundary layer turbulence and the finite-difference vertical spacing used by the NARR to calculate the Richardson number. Examination of boundary layer heights across the Great Lakes region at 0300 UTC revealed a maximum over Lake Erie (1.6 to 1.8 km; not shown) in the vicinity of the tropopause fold. Thus, it is plausible that downward transport of high-momentum air from the tropopause fold region into the

boundary layer could have contributed to the high surface winds in that area, despite the relatively small values of Term C.

In northern Lower Michigan (Fig. 8a), the diffluent/confluent component of the horizontal advective term is the single largest ageostrophic contribution (7.9 m s^{-1}) at 700 hPa in the GEO calculation. In fact, this is the only case for which the isallobaric wind is not the leading-order ageostrophic effect. The calculated wind slightly overestimates the observed wind over the Lake Erie region (Fig. 7a) at 700 hPa (30.8 m s^{-1} and 27.2 m s^{-1}, respectively), but underestimates the magnitude over northern Lower Michigan by approximately 30% (observed wind = 24.8 m s^{-1}).

At 850 hPa, the ageostrophic component is 15-40% of the magnitude of the geostrophic wind depending on the location and details of the calculation ($\mathbf{V_g}$ = 27.0 and 30.2 m s^{-1} in the Lake Erie region (Fig. 7b) and northern Lower Michigan (Fig. 8e), respectively). The isallobaric component (A) is the leading term, followed by the diffluent/confluent component of the horizontal advective term (B2). The match between observed and calculated total wind is nearly perfect across the Lake Erie region, but is underestimated by nearly 33% with respect to magnitude for northern Lower Michigan (observed wind = 27.2 m s^{-1}). The vertical advective term (C) remains a tertiary effect (in the GEO calculations; 2.8 m s^{-1}) but has less influence on the ageostrophic wind at 850 hPa than at 700 hPa.

At 925 hPa, the ageostrophic component is more than 50% of the magnitude of the geostrophic wind in both domains [$\mathbf{V_g}$ = 26.9 and 30.7 m s^{-1} in the Lake Erie region (Fig. 7c) and northern Lower Michigan (Fig. 8f), respectively]. The dominant ageostrophic term in both domains is the isallobaric term (A), followed by the horizontal advective (B1, then B2) and frictional terms (D). Similar to the other levels, the match between the observed wind and the calculated total wind ($\mathbf{V_g} + \mathbf{V_{ag}}$) at 925 hPa (for both direction and speed) is excellent for the Lake Erie region, but our calculations underestimate the magnitude of the total wind by nearly 42% (observed wind = 21.2 m s^{-1}) in northern Lower Michigan. The vertical advective term (C) at 925 hPa is larger in the Lake Erie region than in northern Lower Michigan (~1.5 vs 0.4 m s^{-1}), but contributes less to the ageostrophic wind budget than at 850 and 700 hPa.

The GEO calculations were more accurate than the WND calculations in magnitude (relative error 5.4% vs. 19.2%) and direction (relative error 3.4% vs. 4.3%) for the Lake Erie region. As noted above, both methods were less accurate for northern Lower Michigan, underestimating the wind magnitude by 6-9 m s^{-1}. We infer that the use of the geostrophic wind instead of the full wind in these

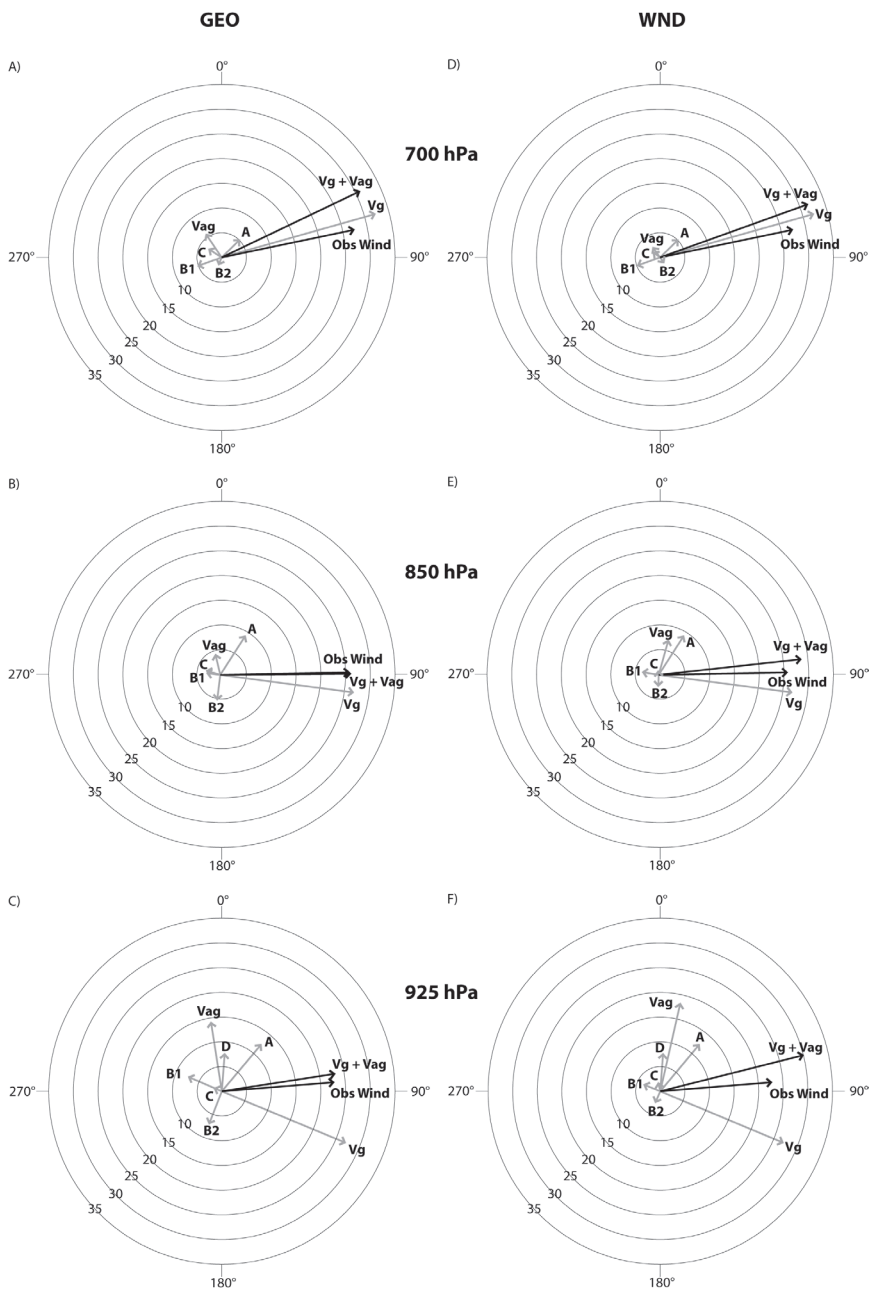

Fig. 7. Calculated geostrophic (Vg) and ageostrophic (Vag) components of the total wind and the observed wind (both in m s^{-1}) for the Lake Erie region at 0300 UTC on 13 November 2003. Calculations of terms B1, B2, and C were performed using both the geostrophic (GEO; left column) and total wind (WND; right column). Winds were calculated at 700 hPa (a and d), 850 hPa (b and e), and 925 hPa (c and f).

calculations is satisfactory, at least for this particular case study.

In summary, the results in Figs. 7 and 8 show that regardless of the location, synoptic situation, pressure level, or details of calculation, the ageostrophic contribution to the total wind in this Great Lakes windstorm is not dominated by any one term. Instead, as the figures illustrate, $\mathbf{V}_{ag}$ is the vector sum of several ageostrophic wind mechanisms.

6. Discussion and Conclusions

This work extends the RM06 analysis via an examination of ageostrophic wind components, in particular a comprehensive numerical comparison of ageostrophic contributions to a non-convective windstorm in the Great Lakes region in November 2003. Our qualitative analysis helps to explain some empirical forecasting rules-of-thumb. Our aggregate numerical results compare extremely well to the observed winds for the Lake Erie region, lending credence to our approach.

We conclude from the numerical results that the isallobaric wind is the leading-order ageostrophic contribution in the November 2003 non-convective high wind event, even in regions where vertical advection might be expected to play a dominant role. The isallobaric wind is generally between 5-12 m s^{-1} in our analysis, considerably less than the 21 m s^{-1} Richwien (1980) calculated for the *Edmund Fitzgerald* storm. However, all other ageostrophic terms analyzed here play non-negligible roles in some circumstances from 700 hPa to the surface. Thus, a main point of our paper is that analyses that focus only on one term, or do not combine vectorially all geostrophic and ageostrophic contributions, are likely to be misleading. The combined effect of the ageostrophic wind terms at all levels was generally to alter the direction of the geostrophic wind rather than to combine with the geostrophic wind to create even higher winds. This is in contrast to Crupi's (2004) analysis of a windstorm in the upper peninsula of Michigan.

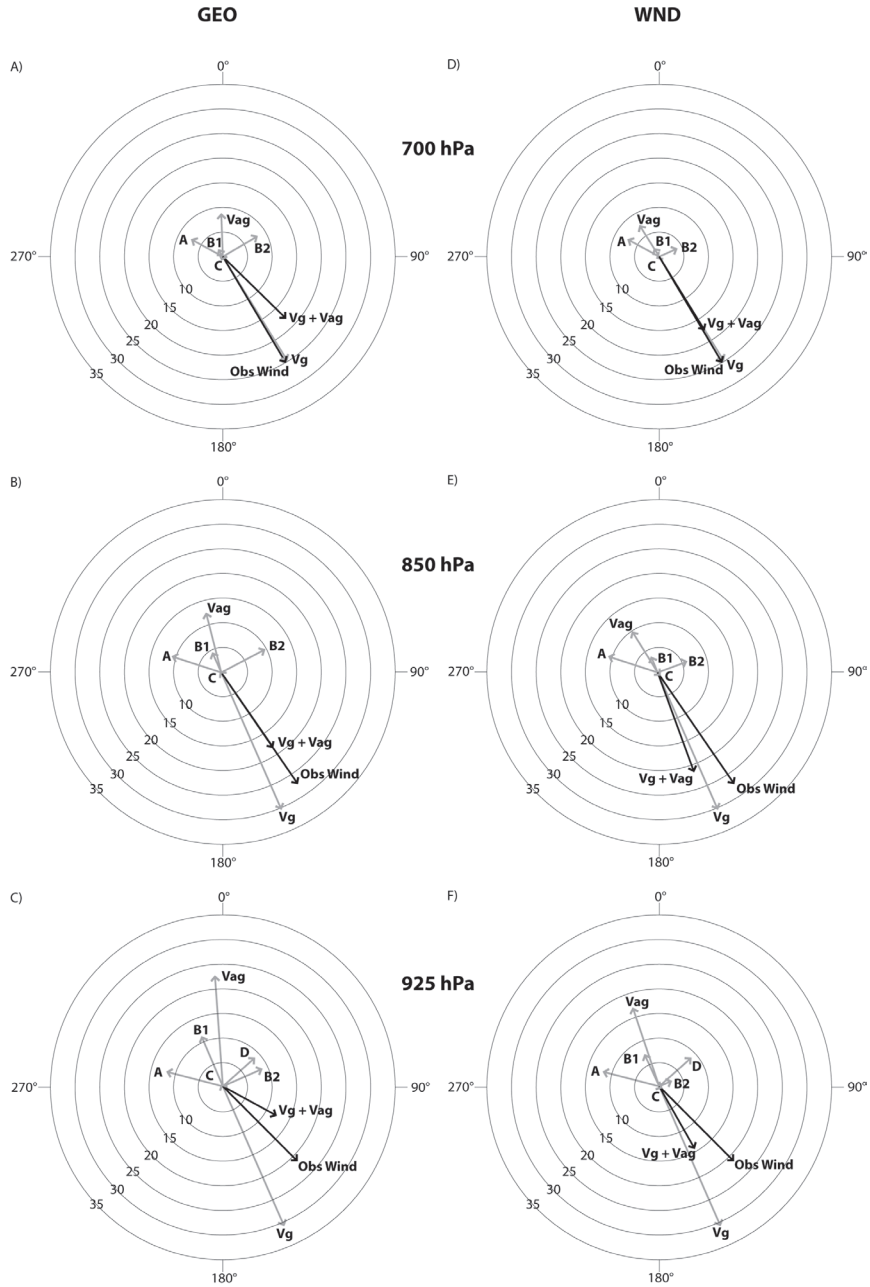

Figure 8. As in Figure 7 except for northern Lower Michigan at 1200 UTC, 13 November 2003.

The explanation for the somewhat less accurate match between calculated and observed wind at 700 hPa in the Lake Erie region, and the much less accurate match in northern Lower Michigan, is not apparent. One possibility is that vertical advective effects are underestimated at 700 hPa over the Lake Erie region. For example, small-scale turbulent mixing via Kelvin-Helmholtz instability, as revealed by low Richardson numbers near 700 hPa in the region of the tropopause fold, may not be adequately captured in our calculations and may require higher-resolution modeling. The inaccuracies over northern Lower Michigan, in contrast, appear to be due to an overestimate of ageostrophic effects. Resolving these discrepancies will be subject of future research.

Additional future work will be devoted to relating our results to Kapela et al.'s (1995) checklist, and developing operational tools that integrate their checklist with our dynamically based analysis.

Authors

Joshua Durkee is an assistant professor in the meteorology program at Western Kentucky University's Department of Geography and Geology. He received a BS in geography from Western Kentucky University, and MS and PhD degrees in geography from the University of Georgia. His research interests include synoptic and mesoscale meteorology / climatology, hydroclimatology, atmospheric circulation and teleconnections, remote sensing and GIS applications in the atmospheric sciences, and education assessment and reform in the atmospheric sciences.

Christopher Fuhrmann is the Regional and Research Climatologist for NOAA's Southeast Regional Climate Center and doctoral candidate in geography at the University of North Carolina-Chapel Hill. His research interests are in synoptic climatology, weather and society, climate and human health, winter weather, and climate variability and change. He holds a BA in geography from UNC-Chapel Hill and an MS in geography from the University of Georgia.

John Knox is an associate professor of geography in the atmospheric sciences program at the University of Georgia in Athens, Georgia. His research interests focus on atmospheric and climate dynamics, including non-convective high winds, clear-air turbulence forecasting and inertial instability. He received a BS in mathematics from the University of Alabama at Birmingham and earned a PhD in atmospheric sciences from the University of Wisconsin-Madison, and was a post-doctoral fellow at Columbia University in conjunction with the NASA/Goddard Institute for Space Studies. Knox has served as an Associate Editor of the *National Weather Digest* and was the 2010 recipient of the T. Theodore Fujita Research Achievement Award from the NWA.

John Frye is an assistant professor of geography and geology at the University of Wisconsin-Whitewater. His research interests are land surface–atmosphere interactions, weather impacts on society, climate variability, and remote sensing applications in meteorology and climatology. He earned a BS in journalism and an MS in geography from Ball State University and a PhD in geography from the University of Georgia.

Acknowledgments

Our sincere thanks to Phil Kurimski, who first directed our attention to this windstorm and whose interest and support have kept us working on it. Stephen Jascourt provided invaluable dynamical insights. Greg Mann and David Schultz gave thoughtful informal reviews that helped enormously in the development of this paper. We thank the *NWD* Chief Editor Gary Ellrod and reviewers Scott Rochette, Robert A. Weisman and Mary Cairns, who helped shape the final paper in numerous ways. Thanks also to the summer research seminar participants at the University of Georgia who commented on this research in its initial stages.

References

Ashley, W. S., and A. W. Black, 2008: Fatalities associated with nonconvective high-wind events in the United States. *J. Appl. Meteor. Climatol.*, 47, 717–725.

Asuma, J. V., 2010: Cool-season high-wind events in the Northeast U.S. M.S. thesis, University at Albany, State University of New York, 117 pp. [Available online at http://cstar.cestm.albany.edu/CAP_Projects/Project17/JAsuma/Asuma_Total_4Oct10_Final.pdf]

Bergmann, J. C., 1998: A physical interpretation of von Kármán's constant based on asymptotic considerations—a new value. *J. Atmos. Sci.*, 55, 3403-3407.

Bluestein, H. B., 1993: *Synoptic-Dynamic Meteorology in Midlatitudes, Volume II: Observations and Theory of Weather Systems*. Oxford University Press, 594 pp.

Browning, K. A., 2004: The sting at the end of the tail: Damaging winds associated with extratropical cyclones. *Q. J. R. Meteorol. Soc.,* 130, 375-399.

Browning, K. A., and R. Reynolds, 1994: Diagnostic study of a narrow cold-frontal rainband and severe winds associated with a stratospheric intrusion. *Q. J. R. Meteorol. Soc.,* 120, 235-257.

Broyden, C. G., 1965: A class of methods for solving nonlinear simultaneous equations. *Math. Comp.*, 19, 577-593.

Crupi, K. M., 2004: An anomalous non-convective high wind episode over Upper Michigan. *Natl. Wea. Dig.,* 28, 3-12.

Danielsen, E. E., 1964: Project Springfield Report. Defense Atomic Support Agency, Washington, D.C., 97 pp. [NTIS AD-607980.]

Djurić, D., 1994: *Weather Analysis.* Prentice-Hall, 304 pp.

Great Lakes Environmental Research Laboratory (GLERL), 2006: Great Lakes storms photo gallery - Great Lakes storm surges November 12-13, 2003. [Available online at: http://www.glerl.noaa.gov/seagrant/glwlphotos/Seiche/1113Storm/November2003.html]

Haltiner, G. J., and F. L. Martin, 1957: *Dynamical and Physical Meteorology.* McGraw-Hill, 470 pp.

Haurwitz, B., 1946: On the relation between the wind field and pressure changes. *J. Meteor.*, 3(3), 95–99.

Holton, J. R., 2004: *An Introduction to Dynamic Meteorology*, 4th ed. Elsevier Academic Press, 529 pp.

Hubert, W. E., and D. Morford, 1987: Great Lakes Forecaster's Handbook, Jet Propulsion Laboratory Contract No. 957762, Ocean Data Systems, Monterey, CA 93490.

Hultquist, T. R., M. R. Dutter, and D. J. Schwab, 2006: Reexamination of the 9-10 November 1975 "*Edmund Fitzgerald*" storm using today's technology. *Bull. Amer. Meteor. Soc.,* 87, 607-622.

Iacopelli, A. J., and J. A. Knox, 2001: Mesoscale dynamics of the record-breaking 10 November 1998 mid-latitude cyclone: A satellite-based case study. *Natl. Wea. Dig*., 25 (1-2), 33-42.

Kapela, A. F., P. W. Leftwich, and R. Van Ess, 1995: Forecasting the impacts of strong wintertime post-cold front winds in the northern Plains. *Wea. Forecasting*, 10, 229-244.

Knox, J. A., 1996: A theoretical and observational study of inertial instability and nonlinear balance. Ph.D. dissertation, University of Wisconsin-Madison, 351 pp. [Available from Department of Atmospheric and Oceanic Sciences, University of Wisconsin-Madison, 1225 W. Dayton St., Madison, WI 53706.]

Knox, J. A., 2004: Non-convective windstorms in the Midwest United States: Surface and satellite climatologies. Preprints, *22nd Conf. on Severe Local Storms*, Hyannis, MA, Amer. Meteor. Soc.

Knox, J. A., J. D. Frye, J. D. Durkee, and C. M. Fuhrmann, 2010: Non-convective high winds associated with extratropical cyclones. *Geography Compass*, in press.

Kurtz, J., and J. Martinelli, 2010: Climatology of cold-season non-convective wind events for the north central Plains. *35th Annual Meeting*, Tucson, AZ, National Weather Association. [Available online at http://nwas.org/meetings/nwa2010/]

Lacke, M. C., J. A. Knox, J. D. Frye, A. E. Stewart, J. D. Durkee, C. M. Fuhrmann, and S. M. Dillingham, 2007: A climatology of cold-season nonconvective wind events in the Great Lakes region. *J. Climate*, 20, 6012–6022.

Mesinger F., G. DiMego, E. Kalnay, K. Mitchell, P. C. Shafran, W. Ebisuzaki, D. Jovic, J. Woollen, E. Rogers, E. H. Berbery, M. B. Ek, Y. Fan, R. Grumbine, W. Higgins, H. Li, Y. Lin, G. Manikin, D. Parrish, and W. Shi, 2006: North American regional reanalysis. *Bull. Amer. Meteor. Soc.* 87, 343-360. [Available online at http://journals.ametsoc.org/doi/pdf/10.1175/BAMS-87-3-343]

Moore, J. T., and G. E. VanKnowe, 1992: The effect of jet-streak curvature on kinematic fields. *Mon. Wea. Rev*., 120, 2429-2441.

National Climatic Data Center (NCDC), 2003: *Storm Data.* Vol. 45, No. 7, 478 pp. [Available online at http://www.ncdc.noaa.gov/oa/climate/sd/]

National Weather Service (NWS), 2005: Summary of natural hazard statistics for 2004 in the United States. [Available online at http://www.weather.gov/os/hazstats.shtml]

Niziol, T. A. and T. J. Paone, 2000: A climatology of non-convective high wind events in western New York State. NOAA Tech. Memor., NWS ER-91, 36 pp. [Available online at http://www.erh.noaa.gov/er/buf/research/webwind/windweb1.htm]

Pauley, P. M., N. L. Baker, and E. H. Barker, 1996: An observational study of the "Interstate 5" dust storm case. *Bull. Amer. Meteor. Soc.,* 77, 693-720.

Pore, A. N., H. P. Perrotti, and W. S. Richardson, 1975: Climatology of Lake Erie storm surges at Buffalo and Toledo. NOAA Tech. Memor., NWS TDL-54, 27 pp. [Available from Techniques Development Laboratory, NWS, SSMC2, Silver Spring, MD 20910]

Reed, R. J., 1990: *Advances in knowledge and understanding of extratropical cyclones during the past quarter century: An overview*. Chapter 3 in Extratropical Cyclones: The Erik Palmén Memorial Volume, C.W. Newton and E.O. Holopainen, Eds., American Meteorological Society, 27-45.

Richwien, B. A., 1980: Isallobaric contribution to a ship's sinking. Preprints, *8th Conf. on Weather Forecasting and Analysis*, Denver, CO, Amer. Meteor. Soc., 52-56.

Rochette, S. M. and P. S. Market, 2006: A primer on the ageostrophic wind. *Natl. Wea. Dig*., 30, 17-28.

Saucier, W. J., 1955: *Principles of Meteorological Analysis*. Dover, 438 pp.

Schultz, D. M., and J. A. Knox, 2007: Banded convection caused by frontogenesis in a conditionally, symmetrically, and inertially unstable environment. *Mon. Wea. Rev.*, 135, 2095-2110.

Schultz, J., and B. Meisner, 2009: The 24 February 2007 north Texas wind and dust storm: An impact weather event. *Natl. Wea. Dig.*, 33, 165-184.

Stull, R. B., 1988: *An Introduction to Boundary Layer Meteorology.* Kluwer Academic, 666 pp.

Uccellini, L. W., 1990: *Processes contributing to the rapid development of extratropical cyclones*. Chapter 6 in Extratropical Cyclones: The Erik Palmén Memorial Volume, C. W. Newton and E. O. Holopainen, Eds., American Meteorological Society, 81-105.